Journal of Membrane Science & Research

journal homepage: www.msrjournal.com

Research Paper

Nanoparticle Separation Using Direct Contact Membrane Distillation and Its Fouling Study

H.Y. Wong[1], K.K. Lau[2], E. Drioli[3], O.B. Seng[1,*]

[1]*School of Chemical Engineering, Engineering Campus, Universiti Sains Malaysia, Seri Ampangan, 14300 Seberang Prai Selatan, Pulau Pinang, Malaysia*
[2]*Department of Chemical Engineering, Faculty of Engineering, Universiti Teknologi Petronas, Bandar Seri Iskandar, 31750, Tronoh, Perak Darul Ridzuan, Malayisa*
[3]*National Research Council, Institute on Membrane Technology (ITM-CNR) c/o University of Calabria - Cubo 17C, 87036 Rende CS, Italy*

ARTICLE INFO

Received 2015-10-06
Revised 2015-11-06
Accepted 2015-11-08
Available online 2015-12-15

KEYWORDS

Direct contact membrane distillation
DCMD
Nanoparticles separation
Flux
Rejection

GRAPHICAL ABSTRACT

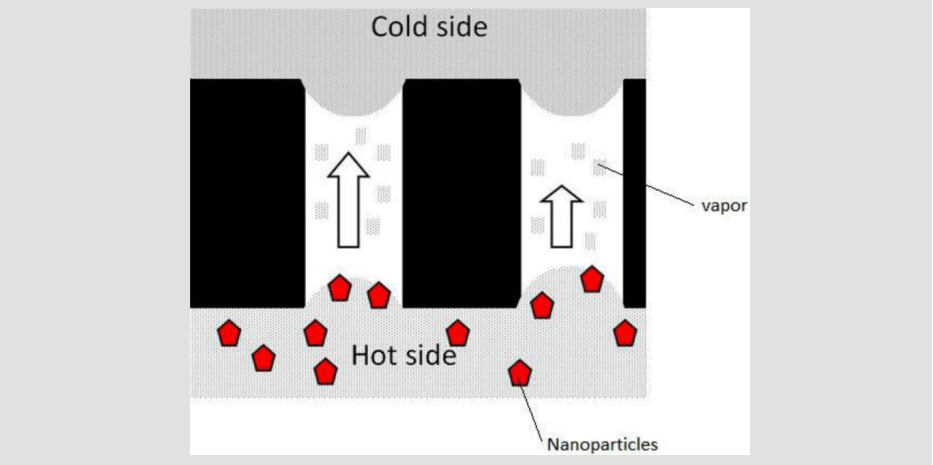

HIGHLIGHTS

- Nanoparticles could be effectively separated via membrane distillation.
- Presence of nanoparticles could enhanced the vaporization of water.
- Membrane distillation has better antifouling properties compared to microfiltration.

ABSTRACT

Direct contact membrane distillation (DCMD) which emerges as an alternative separation technology can effectively perform a colloidal separation process under thermal driven force. DCMD is capable of extracting pure water from aqueous solutions containing non-volatile nanoparticles through the hydrophobic microporous membrane when a vapour pressure difference was established across the membrane. This work aims to study the efficiency of the MD process in separating TiO_2 nanoparticles. It was interesting to find out that below 1.0 g/L TiO_2 concentration, no sign of flux reduction was noticed. It is indicated that the pore blocking phenomenon was not significant. However, as concentration exceeding 1.0 g/L, the flux started to decline due to the resistance of the gelation layer which impeded water from flowing through the membrane. The blocking law analysis showed that the cake layer was developed within 3 hours of operation. At higher feed velocity, the flux declination problem could be solved due to the surface scouring effect.

1. Introduction

Nanoparticles in suspension exerted separation and recovery difficulties due to their smaller size. Nanoparticle isolation is an important process as the release of such particles into water streams might bring adverse effects towards human health. Thus it is essential to adopt an effective separation process to isolate the nanoparticles from the discharged stream. Available nanoparticles separation techniques include centrifugation [1], sedimentation [2], electrophoresis [3], diafiltration [4] and magnetic separation [5]. In spite of their superior separation efficiency, the methods reported above are normally operated in laboratory or pilot scale due to their limited capacity. On the other hand, the membrane filtration process which requires smaller foot prints is an attractive alternative method used to separate the nanoparticles from the treated water. Most of the examples of nanoparticle separation (in particularly TiO_2)

* Corresponding author at:Phone: +6045996418; fax: +6045996908
E-mail address: chobs@usm.my (O. Boon Seng)

using membrane technology can be seen from the hybrid photocatalytic membrane reactor. In such reactors, the suspended TiO_2 catalyst could degrade the pollutants such as dye while retaining them within the reactor. However, fouling is a serious problem for such pressure driven membrane processes [6]. The recent studies on the thermal driven membrane separation process such as membrane distillation (MD) showed better fouling resistance compared to the pressure driven membrane. This is because the particles do not contact the membrane surface directly due to the low surface energy of the membrane material. In view of this, MD is widely applied to separate the dye and catalyst from the treated water [7-9]. An important advantage of membrane distillation is that the membrane fouling phenomenon due to the presence of particles in the feed is insignificant. It was found that the presence of pure TiO_2 in the feed solution did not affect the permeate flux, regardless of the TiO_2 concentration applied [7-11]. In the absence of high pressure, pore blocking can be avoided and thus the main factor which is responsible for membrane fouling is excluded. However, it is important to note that the TiO_2 nanoparticles concentration was usually limited to 5 g/L or lower [12-14].

In spite of its many applications of MD in catalyst removal, its direct application to isolate the nanoparticle with the defined membrane pore to particle size ratio, hitherto, remains remarkably scarce. The pool of literatures seldom reported the actual or hydrodynamic size of the catalyst in the suspension as many nanoparticles will tend to aggregate in the medium during the separation. The formation of cake layer will therefore impair the separation efficiency and cannot be ignored. In this study, the effectiveness of MD in separating TiO_2 nanoparticles at a wider range of concentrations was investigated and their fouling phenomenon and mechanisms were evaluated.

2. Materials and methods

2.1. Materials

Commercial hydrophobic supported polytetrafluoroethylene (PTFE) membranes with a nominal pore size of 0.2 µm supplied by Sterlitech Corporation were used in the experiment. The TiO_2 slurry solution (X-500) to be separated in the MD process was purchased from TitanPE Technologies, Inc. Perfluorothers used as wetting liquid for porometer were purchased from CNG Instruments while 2-butanol that acts as wetting liquid for porosity testing was purchased from Merck.

2.2. Nanoparticle and membrane characterization

The zeta potential of TiO_2 nanoparticles was determined by using the Laser Doppler Micro-electrophoresis technique (Malvern Zetasizer Nano ZS90) at 25 ºC. The size of TiO_2 nanoparticles was analysed based on the Dynamic Light Scattering method using the same equipment.

A digital micrometer with 0.1 µm accuracy was used to check the thickness of the membrane. The hydrophobicity of the membrane which is indicated by a contact angle was measured using a Model 300 Advanced Goniometer (Rame-Hart Instrument Co., USA) based on the sessile drop method. A Capillary Flow Porometer (Porolux 1000, Benelux Scientific, Germany) was used to determine the pore size distribution and mean pore size of the membrane via the bubble point method. In addition, the Capillary Flow Porometer was also applied to determine the Liquid Entry Pressure (LEP) of the membrane using pure water as wetting liquid. The thermal conductivity of the membrane was measured using a Hot Disk Thermal Constant Analyzer (TPS 2500S) which applies the Transient Plane Source (TPS) technique. The porosity of the membrane was determined through the mass difference technique. The morphology of the surface of the membrane was studied using a Scanning Electron Microscopy (JEOL JSM 6460 LA) while the composition of deposition on the membrane surface was analyzed using Energy Dispersive X-ray (Oxford INCA 400).

2.3. Experimental Set up

Figure 1 illustrates the experimental set up of the membrane distillation process. The performance of the DCMD processes were evaluated using a flat sheet membrane module/cell made from acrylic plastic. The membrane was maintained in a horizontal position during the whole experimental run. Two flow channels were engraved in each of the acrylic blocks which consists of inlet and outlet at both feed and permeate side. The effective area of the membrane being used in the experiment is 16 cm × 6 cm, whereas the depth of the channel on each side is 1.5 cm. The feed solution was heated to the desired temperature by placing it in a hot water bath (Protech HC-10). The feed solution was continuously pumped from the feed reservoir through the horizontally oriented membrane cell and returned to the reservoir by using a speed adjustable peristaltic pump (Masterflex L/S Cole-Parmer). For the permeate stream, the distillate was continuously recirculated within the permeate loop and was cooled to the desired permeate temperature using a chiller (Huber minichiller). The permeate reservoir is a jacketed flask that allows the overflow of excess water which results from the vapor permeation process. The overflow of permeate was continuously weighted on an electronic balance (A&D company limited FX-3000i) and the data is directly transmitted to the computer. The turbidity was measured by using the turbidity meter (HANNA instruments HI 93703) in order to determine the TiO_2 content at the permeate side. The flux was calculated as the weight of permeate water collected over time and per unit area of the membrane (96 cm^2). Pressures of feed and permeate side were monitored by using pressure gauges (Unijin EN837-1). While for the flow rates, they were measured using a flow meter (Dwyer).

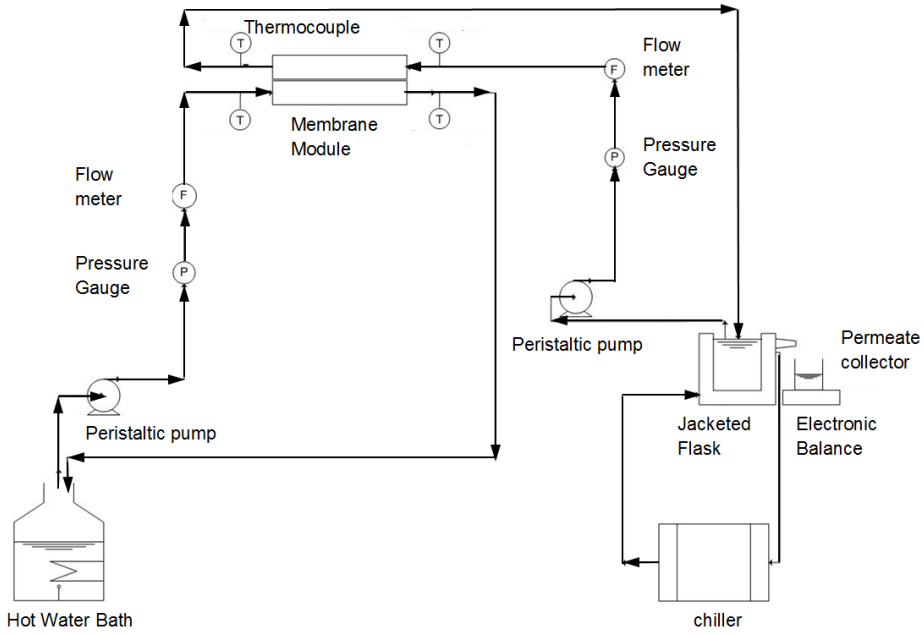

Fig. 1. Schematic diagram of DCMD experimental setup.

The effect of feed TiO_2 concentration on the permeate flux was investigated within the range of 0.01 g/L to 9 g/L. Each of the experiments was carried out at a fixed flow rate of 1.4 L/min (or 0.297 m/s) for both sides. This is while the feed and permeate inlet temperatures were maintained at 70 °C and 19 °C, respectively. The effect of flow rate on the MD system with the presence of TiO_2 was done by comparing the system of two different flow rates which were 0.3 L/min (0.064 m/s) and 1.4 L/min (0.297 m/s). The concentration was fixed at 9.0 g/L at a constant temperature of 70 °C and 19 °C for the hot and cold stream, respectively. The MD process was carried out for a duration of 12 hours.

The experimental performance of the membrane was evaluated based on the permeation flux and solute rejection of TiO_2. The permeation flux of the membrane, J was determined by the following relation:

$$J = \frac{V}{At} \quad (1)$$

where J is permeation flux (L/m^{2}h), V is permeate volume (L), A is membrane surface area (m^2), and t is time (h).

Rejection of the nanoparticle (R) was calculated from the feed and permeates concentrations using the following equation:

$$R = \left(1 - \frac{c_p}{c_f}\right) \times 100\% \quad (2)$$

where R is the particle rejection (%), c_p is the concentration of the particle in the permeate solution and c_f is the concentration of the feed solution. The calibration curve of turbidity (NTU) versus concentration of TiO_2 was constructed to determine the membrane rejection efficiency. Through the calibration curve, the concentrations of nanoparticles in the feed or permeate were obtained by comparing it with a set of standard samples with known concentrations.

3. Results and discussion

3.1 Nanoparticle characteristics (TiO_2)

The zeta potential of TiO_2 nanoparticles was -46.5 mV which indicated that the suspension was in a stable form to withstand agglomeration. The stable suspension was generally taken at a value higher than +30 mV or lower than -30 mV. Stable suspension was important for the subsequent experiment to evaluate the fouling behaviour of the membrane as it is crucial to maintain the consistent particle size to pore size ratio. The particle size (hydrodynamic diameter) has the average value of 37.35 nm with a good particle size distribution (PdI value = 0.252).

3.2. Membrane characteristics

Table 1 lists the characteristic of the commercial PTFE membrane. The thickness of the membrane was around 135 µm. The contact angle of the membrane was 118.7°±2° while the LEP was 2.35 bar. The membrane appeared to be highly hydrophobic due to the high values of contact angle and LEP. The thermal conductivity of the membrane was found to be 0.04867 W/m.K which is within the acceptance range used for MD [15]. The porosity of the membrane was around 83% which was rather satisfying since the membrane with higher porosity (70-80%) tends to exhibit greater surface area for water evaporation.

Table 1
Characteristics of PTFE membrane through different tests.

Characteristics	Values
Thickness	135±2 µm
Contact angle	118.7°±2°
LEP	2.35±0.23 bar
Thermal conductivity	0.0487±0.0007 W/m.K
Porosity	83±3%
Mean pore size	0.23±0.03 µm

Figure 2 illustrates the pore size distribution of the membrane determined via the Capillary Flow Porometer. The membranes have very narrow pore size distribution with a mean pore size of 0.23 µm. It was stated that in order to prevent the wetting phenomenon in the DCMD process, the membrane pore size should be smaller than 0.5 µm [16]. The narrow pore size distribution exhibited by the commercial PTFE membrane is mostly favorable as it provides a better estimation of permeate flux during the MD process.

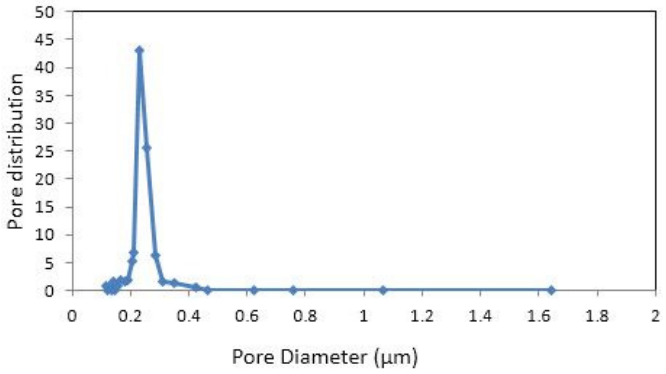

Fig. 2. Pore size distribution of PTFE membrane.

3.3. Effect of Feed (TiO_2) Concentration

The effect of TiO_2 feed concentrations towards flux is shown in Figure 3. It was observable that at a low dosage of TiO_2, the flux seems not to be affected by the addition of TiO_2. In fact, a total of 4.6 % flux enhancement was achieved for the system with 1.0 g/L TiO_2 compared to the pure water. This is probably due to the enhanced thermal conductivity of the fluid when the nanoparticle was being added [17-18]. Suspension of nanoparticles can improve the heat transfer characteristics of the fluid as the suspended nanoparticles increase the surface area and heat capacity of the fluid. The surface area of particles is very important in determining the thermal conductivity of fluid since a larger surface area means more area is available for heat transfer to occur.

The heat transfer enhancement mechanism by the nanoparticle is due to two main aspects. Initially, the suspended particles with a large total surface area provide more surfaces for heat transfer and this will increase the thermal conductivity of the mixture. A recent study by Zhang et al. [19] shows that nanoparticles could enhance the evaporation of liquid according to the different chemistry, size and structure of the particle (see Ref. [19]). The weak absorption sites on the particles that half float on the liquid surface are responsible for the facilitated evaporation of the liquid molecules. Secondly, nanoparticles are able to enhance heat transfer of fluid by causing chaotic movement which increases the fluctuation and turbulence of the fluid and subsequently accelerates the energy exchange rate in the fluid [20]. The nanoparticles which were suspended within the fluid will undergo continuous collisions with the base fluid molecule and induce the mixing effect which enhanced the convective heat transfer within the fluid.

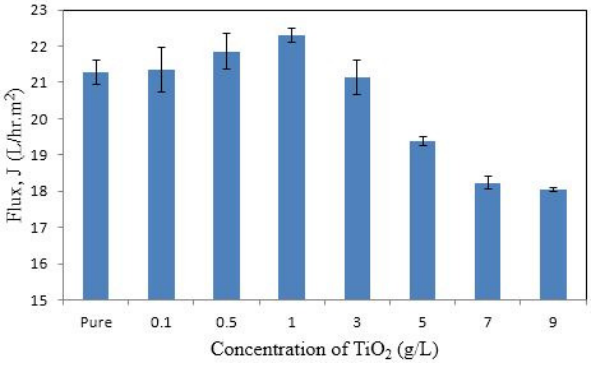

Fig. 3. Effect of TiO_2 concentration on flux of membrane.

However, as the concentration of TiO_2 exceeded 1.0 g/L, the flux started to decline and fell to the value lower than the pure fluid at a concentration of 3 g/L and above. Flux declination was more obvious as the concentration

reaches 5 g/L where the flux declined from 21.15±0.53 L/hr.m^2 to 19.38±0.14 L/hr.m^2 for a concentration of 3 g/L and 5 g/L, respectively. A further increase of TiO_2 to 9 g/L resulted in flux as low as 18.05±0.05 L/hr.m^2. The obtained results contradict the findings of other researchers who showed that regardless of TiO_2 concentration, the permeate flux was not affected [7-10]. This phenomenon is most likely caused by the formation of a gelation layer (cake layer) on the surface due to the higher TiO_2 concentrations. The cake layer exerted higher flow resistance to the water vapor and thus reduced the membrane flux. This hypothesis could be proven by the following section, whereby increasing the flow velocity could increase the flux if the cake layer resistance is the reason of flux reduction.

3.4. Effect of feed flow rate

Membrane distillation was performed at two different extreme flow rates/velocities which were 0.3 L/min (0.064 m/s) and 1.4 L/min (0.297 m/s) to study the fouling phenomena on the membrane surface. All the separation processes were carried out using 9.0 g/L of TiO_2. The experiments were carried out for 12 hours in order to examine the fouling tendency and rejection rate in separating the colloidal suspension. It can be observed from Figure 4 that at 0.297 m/s, the flux was almost constant showing no significant sign of fouling. On the other hand, the flux was found to decrease with increasing time at a lower velocity of 0.064 m/s. A total of 40% drop in flux from 10.75 L/hr.m^2 to 6.39 L/hr.m^2 was noticed for MD separation at 0.064 m/s with the flux depleted linearly during the operation. The flux depletion in this case was caused by cake layer deposition as proposed above and this could be clearly seen from the membrane surface where a gelation layer was formed after the operation (see Figure 5). The high flow rate which has a better mixing and swirling effect reduced the accumulation of nanoparticles on the membrane surface via the shearing effect. Thus, a high flow rate is essential in preventing the fouling problem (cake layer formation) in the DCMD process.

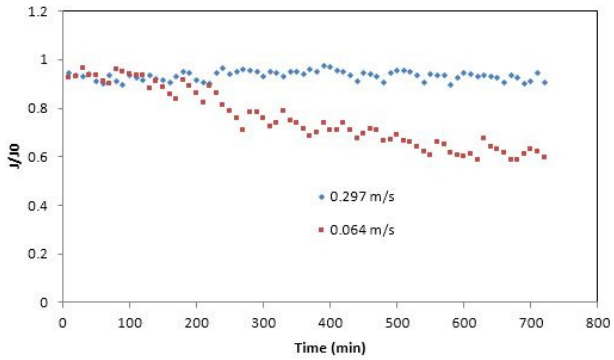

Fig. 4. J/J_o as function of time for membrane distillation at different flow rate.

The rejection efficiencies of MD were evaluated based on the turbidity of the permeates. For the MD process at 0.064 m/s, the turbidity of the permeate was as low as 0.058 FTU which is equivalent to the concentration of 0.0046 g/L TiO_2. The obtained results showed that membrane distillation can retain more than 99.9 % TiO_2 in the suspension. While for the MD process at 0.297 m/s, the average turbidity was around 0.63 FTU which represents the concentration of 0.021 g/L TiO_2. Even though the operating pressures for both sides were well below 0.5 bars, at a higher flow rate, the rejection was slightly dropped to 99.76%. The poorer rejection is due to the possibility of the localized pressure build up on the membrane surface which pushed the TiO_2 to penetrate the bigger pore size (around 0.4 µm) with lower LEPw.

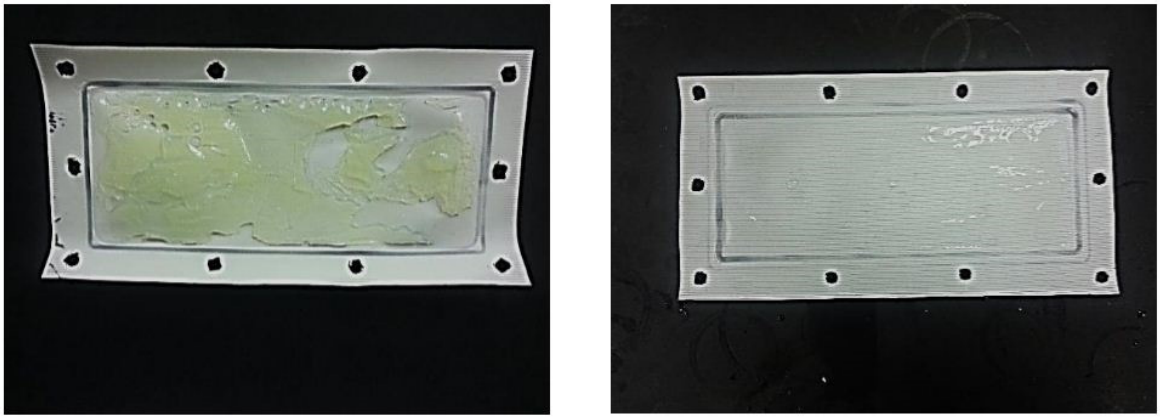

Fig. 5. Gelation layer on membrane surface at inlet velocity of (a) 0.064 m/s and (b) 0.297 m/s.

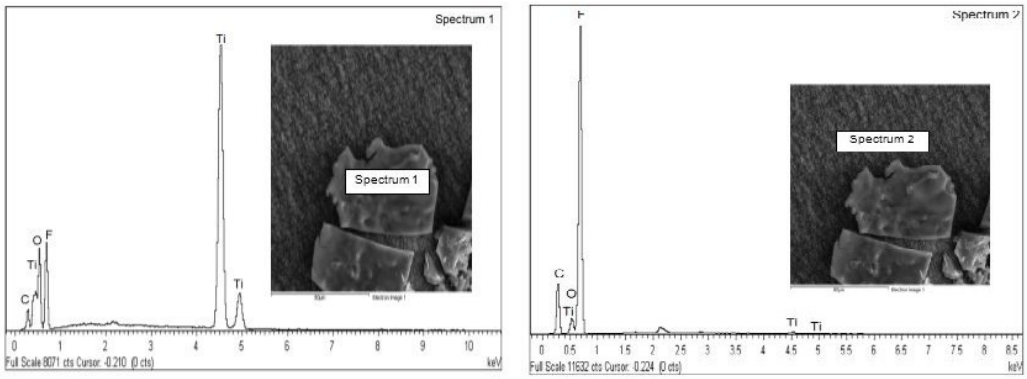

Fig. 6. SEM and EDX images of the membrane surface.

3.5. Nanoparticles fouling phenomenon

The presence of TiO_2 on the membrane surface was examined using SEM-EDX analysis and the results are shown in Figure 6. The membranes being examined were used in the MD separation process in separating 9.0 g/L concentration of TiO_2 for a duration of 12 hours. The SEM-EDX analysis

showed that the deposition on membrane surface contained C, O, F, and Ti. Spectrum 1 which represents the observable TiO_2 deposit on the membrane surface showed atomic percentages of 9.21 % (C), 31.90 % (O), 43.94 % (F), and 14.95 % (Ti). The elements such as C and F indicated the polytetrafluoroethylene (PTFE) membrane, while O and Ti proved the existence of TiO_2 on the membrane surface. While for spectrum 2 (membrane surface with no observable deposit materials), atomic percentages of each element were 33.13 %(C), 3.77 % (O), 62.96 % (F), and 0.14 % (Ti). Only 0.14 % of Ti was detected on the membrane surface, so it can be concluded that TiO_2 pore blocking was not a serious problem for the MD system due to its lower surface energy that mitigates TiO_2 penetration. Thus, it can be deduced that the flux decline in the DCMD process was due to the colloidal fouling which was caused by the cake layer formation on the membrane surface. This cake layer impeded the water from flowing through the membrane and subsequently reduced the permeate water flux.

3.6. Investigation on fouling mechanism

The fouling mechanism of membrane distillation (MD) at lower flow rate and high TiO_2 loading was predicted using the Blocking filtration law. The type of fouling was considered based on the value of parameter n in the following equation [21]:

$$\frac{d^2t}{dV^2} = k\left(\frac{dt}{dv}\right)^n \tag{3}$$

where k and n are the parameters which depend on the characteristics of particle and filtration medium. The type of foulings are classified as cake layer formation, intermediate blocking, standard (pore) blocking and complete blocking for n = 0, 1, 1.5 and 2, respectively.

The results in Figure 7 and 8 show that for filtration time within the first 1.5 hr, the curve best fits to the intermediate blocking (n=1) with R^2 = 0.9381 and for the subsequent filtration from 1.5 hr to 3.0 hr, again the intermediate blocking showed the best fit with R^2=0.9951. After 3 hours of operation, it seems that the fouling mechanism changed from intermediate blocking to cake layer fouling (n=0) with R^2= 0.9991. These observations further supported our hypothesis that although TiO_2 suspension was colloidally stable at 9.0 g/L, upon filtration, particle aggregation actually took place immediately and partially block the passage of the vapor. At prolonged operation (>3 hours), the aggregated particles started to form the cake layer on the membrane surface to further reduce the vaopr permeation.

It is also important to note that at higher operating hours, the intermediate pore blocking could not be totally ruled out as the pore block (standard block) mechanism also recorded high in the regression (R^2=0.9978). Overall, the detrimental fouling effect is unavoidable for high concentration particle separation using MD.

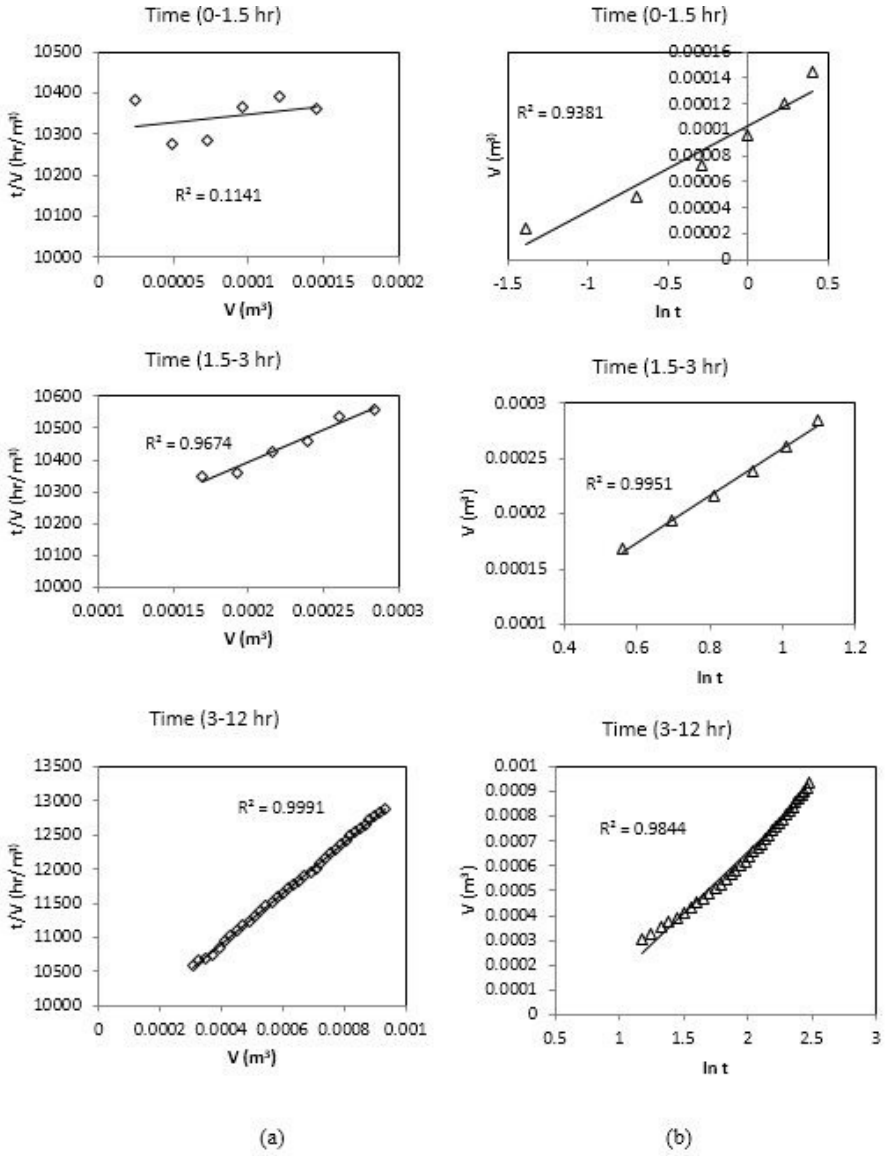

Fig. 7. Plots of (a) *t/V* versus ln *t* (n=0, Cake layer) and (b) *V* versus ln *t* (n=1, intermediate blocking) within 12 hours operation.

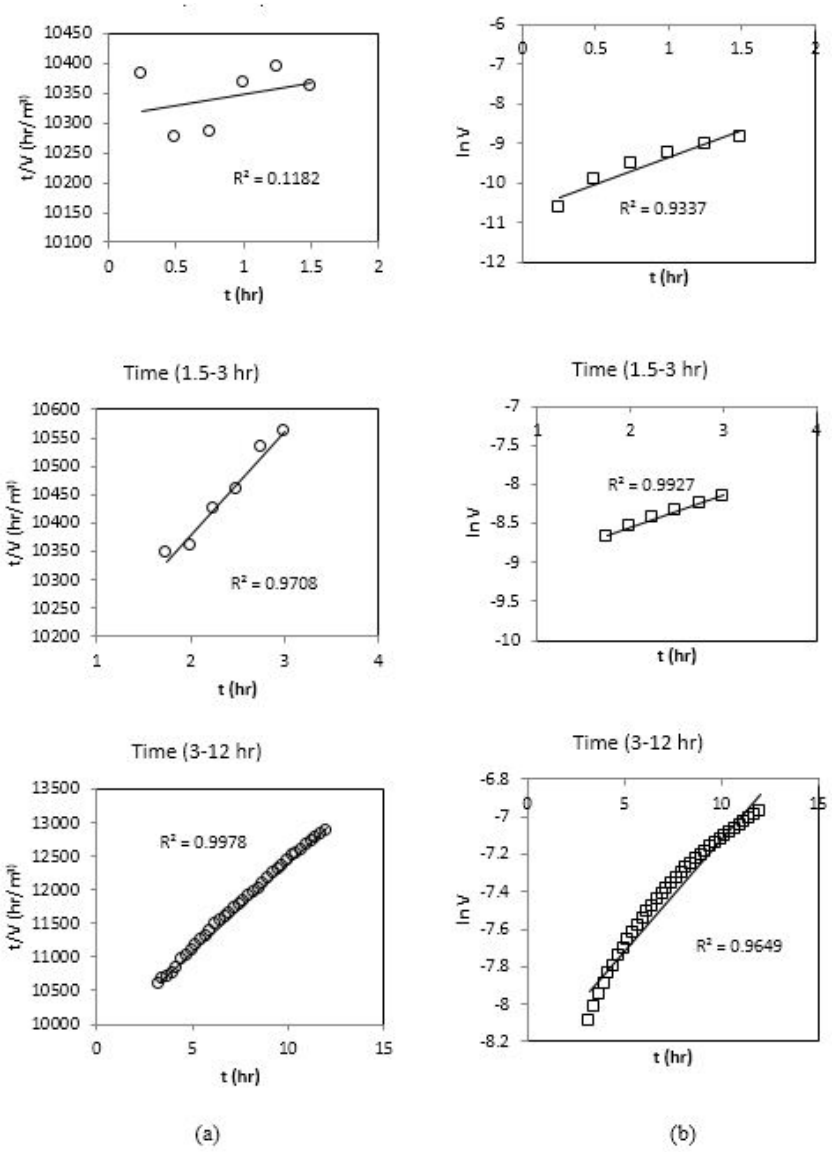

Fig.8. Plots of (a) *t/V* versus *t* (n=1.5, standard blocking blocking) and (b) ln *V* versus *t* (n=2, complete blocking) for 12 hours operation.

4. Conclusion

The presence of nanoparticles in the water has a mixed effect towards the flux of the membrane. When the concentration of TiO_2 was below 1.0 g/L, the flux tends to increase as the concentration increased. This is due to the improved heat transfer by the nanoparticles which subsequently improve the permeate flux. On the other hand, as concentration of nanoparticles exceeded 1.0 g/L, the flux starts to deteriorate rapidly and drop to a value lower than the pure water flux. This was due to the formation of the TiO_2 gel layer on the membrane surface which impeded the vapor permeation. However, it was proven that the flux reduction caused by gel layer deposition could be mitigated at higher feed velocity. The TiO_2 rejection efficiency through the MD process was more than 99% which is less susceptible to the pore blocking phenomenon.

Acknowledgement

The authors would like to thank Ministry of Higher Education, Malaysia for financially support this research through the FRGS grant (203/PJKIMIA/6071252) and Universiti Sains Malaysia for bridging the collaboration works with Prof Enrico Drioli via the IReC grant (1002/PJKIMIA/910409).

References

[1] O. Akbulut, S.R.Mace, R.V. Martinez, A.A., Kumar, Z. Nie, M.R.Patton, G.M.Whitesides, Separation of nanoparticles in aqueous multiphase systems through centrifugation. Nano Lett. 12 (2012) 4060-4064.
[2] P. Fernåndez-Ibånez, Blanco, J., S.Malato, F.J.D.L., Nieves, Appliction of the colloidal stability of TiO2 particles for recovery and reuse in solar photocatalysis. Water Res. 37 (2003) 3180-3138.
[3] W.M. Hwang, C.Y.Lee, D.W.Boo, J.G.Choi, Separation of nanoparticles in different sizes and compositions by capillary electrophoresis. Bulletin-Korean Chem. Society 24 (2003) 684-686.
[4] S.F. Sweeny, G.H. Woehrle, J.E. Hutchison, Rapid purification and size separation of gold nanoparticles via diafiltration, J. American Chem. Society 128 (2006) 3190-3197.
[5] W. Yantasee, C.L. Warner, T. Sangvanich, R.S. Addleman, T.G. Carter, R.J. Wiacek, G.E. Fryxell, C. Timchalk, M.G. Warner, Removal of heavy metals from aqueous systems with thiol functionalized superparamagnetic nanoparticles, Environ. Sci. Technol. 41 (2007) 5114-5119.
[6] C. Mustapha, D. Benamar, Study on Removal Efficiency of Natural Organic Matter and Lead Metal Solution Using Nanofiltration Membrane, J. Chromatography Sep. Techniq. 3 (2012) 142-145.
[7] S. Mozia, A.W. Morawski, Hybridization of photocatalysis and membrane distillation for purification of wastewater, Catal. Today 118 (2006) 181-188.
[8] S. Mozia, M. Tomaszewska, A.W. Morawski, A new photocatalytic membrane reactor (PMR) for removal of azo-dye Acid Red 18 from water, Appl. Catalysis B: Environmental 59 (2005) 131-137.

[9] S. Mozia, M. Tomaszewska, A.W. Morawski, Removal of azo-dye Acid Red 18 in two hybrid membrane systems employing a photodegradation process, Desalination 198 (2006) 183-190.
[10] S. Mozia, A.W. Morawski, M. Toyoda, T. Tsumura, Effect of process parameters on photodegradation of Acid Yellow 36 in a hybrid photocatalysis–membrane distillation system, Chem. Eng. J. 150 (2009) 152-159.
[11] J. Grzechulska-Damszel, M. Tomaszewska, A.W. Morawski, Integration of photocatalysis with membrane processes for purification of water contaminated with organic dyes, Desalination 241 (2009) 118-126.
[12] S.A. Lee, K.H. Choo, C.H. Lee, H.I. Lee, T. Hyeon, W. Choi, H.H. Kwon, Use of Ultrafiltration Membranes for the Separation of TiO2 Photocatalysts in Drinking Water Treatment, Ind. Eng. Chem. Res. 40 (2001) 1712-1719
[13] K. Azrague, P. Aimar, F. Benoit-Marquie´, M.T. Maurette, a new combination of a membrane and a photocatalytic reactor for the depollution of turbid water, Appl. Catal. B: Environmental 72 (2007) 197–204.
[14] S. Mozia, Application of temperature modified titanate nanotubes for removal of an azo dye from water in a hybrid photocatalysis-MD process, Catal. Today 156 (2010) 198–207.
[15] M. Khayet, T. Matsuura, Membrane distillation principles and applications, Amsterdam: Elsevier, 2011, pp. 36.
[16] S. Bonyadi, T.S. Chung, Flux enhancement in membrane distillation by fabrication of dual layer hydrophilic–hydrophobic hollow fiber membranes, J. Membr. Sci. 306 (2007) 134-146.
[17] S.M.S. Murshed, K.C. Leong, C. Yang, Enhanced thermal conductivity of TiO_2—water based nanofluids, Int. J. Thermal Sci. 44 (2005) 367-373.
[18] S. Kakaç, A. Pramuanjaroenkij,, Review of convective heat transfer enhancement with nanofluids, Int. J. Heat Mass Transfer 52 (2009) 3187-3196.
[19] W. Zhang, R. Shen, K. Lu, A. Ji, Z. Cao, Nanoparticle enhanced evaporation of liquids: A case study of silicone oil and water, AIP Adv. 2 (2012) 1-10.
[20] L. Godson, B. Raja, D. Mohan Lal, S. Wongwises, Enhancement of heat transfer using nanofluids—An overview, Renew. Sustain. Energy Rev. 14 (2010) 629-641.
[21] R.S. Juang, S.H. Lin, L.C. Peng, Flux decline analysis in micellar enhanced ultrafiltration of synthetic waste solutions for metal removal, Chem. Eng. J. 161 (2010) 19-26.